Signature: © Pol J Radiol, 2016; 81: 310-316
DOI: 10.12659/PJR.897022

Polish Journal of Radiology
www.PolRadiol.com
ORIGINAL ARTICLE

Received: 2015.12.08
Accepted: 2015.12.15
Published: 2016.07.01

Authors' Contribution:
A Study Design
B Data Collection
C Statistical Analysis
D Data Interpretation
E Manuscript Preparation
F Literature Search
G Funds Collection

The Avaibility of Strain Elastography in a Hydatid Cyst – Interobserver Study

Mahmut Duymuş[1ABCDEF], Mehmet Sait Menzilcioğlu[1AEF], Mustafa Gök[2ABEF], Ahmet Erdem[3BDF], Serhat Avcu[1E], Adem Kırış[3E]

[1] Department of Radiology, Gazi University, Faculty of Medicine, Ankara, Turkey
[2] Department of Radiology, Adnan Menderes University, Faculty of Medicine, Aydın, Turkey
[3] Department of Radiology, Kafkas University, Faculty of Medicine, Kars, Turkey

Author's address: Mahmut Duymuş, Department of Radiology, Gazi University, Faculty of Medicine, Bahçelievler, Ankara, Turkey, e-mail: mahmutduymush@gmail.com

Summary

Background: To differentiate the hydatid cyst (HC) types by ultrasound elastography using two different sizes (4 mm and 8 mm) of the region of interest (ROI) and asking two different radiologists (interobserver) for their opinion.

Material/Methods: Patients with HC were evaluated by USG elastography. The statistical anayses were performed using *Strain index (SI)* which is the unit of strain elastography.

Results: A total of 26 out of 33 patients were female, and 7 were male. The mean age was 38.85±17.62 (range from 10 to 72 years). Type I: 6, Type 2: 6, Type III: 6, Type IV: 11, Type V: 4. There was no significant difference in HC *SI* (regardless of types) between O1 and O2, and 4-mm and 8-mm ROI ($p>0.05$). There was no statistically significant difference between *SI* of HC types of interobservers (O1–O2) and ROI sizes (4–8 mm) ($p>0.05$ for all parameters). The highest correlation between HC types and ROI sizes was in ROI size of 4 mm.

Conclusions: The correlation between *SI* and types was reliable in standard-applied 4-mm ROI. There was no statistically significant difference between interobservers in *SI* values. Thus, elastography tecnhnique is objective for HC but not appropriate to differentiate the types.

MeSH Keywords: Echinococcosis, Hepatic • Elasticity Imaging Techniques • Liver Diseases, Parasitic

PDF file: http://www.polradiol.com/abstract/index/idArt/897022

Background

Hydatid Cyst (HC) is a parasitic and endemic public health problem mostly seen in the Eastern region of Turkey, usually affecting the liver. HC is divided into five types (Type I, II, III, IV, and V) according to its contents, by Gharbi [1]. Type I is a pure cystic and Type V is a pure calcific lesion. The other types range from pure cyst to pure calcific. Both ultrasound (USG) and computed tomography (CT) are used in the differentiation of these types, and the treatment changes depending on the type.

Elastography was first developed by Ophir et al. in 1990–1991 [2–4]. Tissue compression applied by USG probe, is the principle of strain elastography. The compression produces changes in the size and shape of the lesion, i.e. *Strain Index (SI)* [4–7]. Many different types of diseased organs are potential candidates for elastography evaluation. The most appropriate organs are those to which pressure can be applied. Malignant tumoral lesions usually tend to be harder than those of adjacent normal tissue, thus elastography allows to differentiate the malignant lesions using strain. Masses and normal parenchyma of the breast, thyroid, lymph nodes, kidneys and prostate have already been studied with US elastography [2,4,8,9]. However, in recent times USG elastography has been used in the liver. Some studies focused on the normal liver parenchymal while some other studies focused on fibrosis and masses of that organ [10–13].

In this prospective descriptive study, we evaluated the *SI* of HC types using two different sizes (4 mm and 8 mm) of the

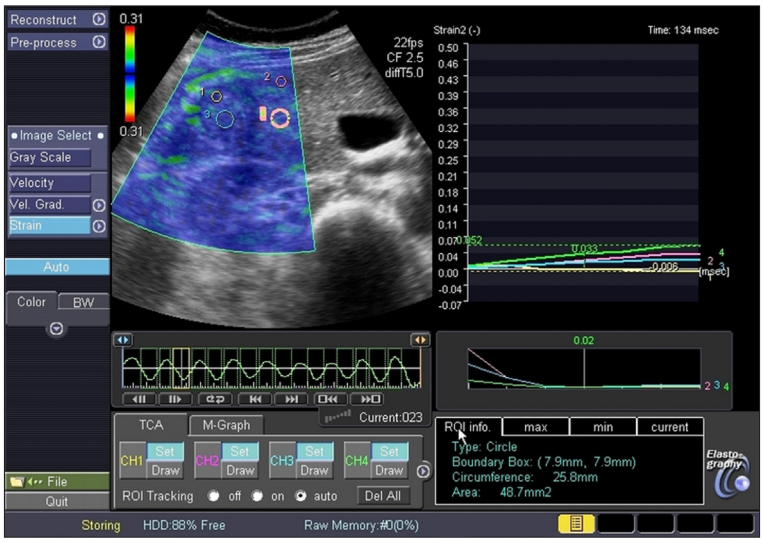

Figure 1. The image shows an ultrasound screen while the elastography programme is active. In the center of the screen, gray-scale USG image and color-coded elastography of the liver and type IV Hydatid Cyst (HC) are seen. There are four different circles in the color-coded region which are regions of interest (ROI). The smaller ones are 4 mm and the bigger ones are 8 mm in diameter. The ROIs have numbers. Number 1 indicates a 4-mm ROI in HC (reference ROI), number 2 indicates a 4 mm ROI in the normal liver parenchyma, number 3 indicates an 8-mm ROI in HC and number 4 indicates an 8-mm ROI in the normal parenchyma. Under the liver image, there is a regular sinusoidal wave. This wave shows the compression and decompression phases of the probe. The compression phase is above the baseline and the decompression phase is below the baseline. In this image the measurements are obtained in the second decompression phase. There are four boxes under the wave, where applications of ROIs are set. On the right side of the screen, there are two graphics indicating the numerical values of the strains obtained with ROIs. Four lines belong to four ROIs. Under the graphic line there are roman numericals seen in the black box. These are numerical values of the strains. We used these numbers in the statistical analysis.

region of interest (ROI) and asking two different radiologists (interobserver) for their opinion, because theoretically the *SI* of HC tended to increase from Type I to Type V due to calcification. We expected that *SI* of all V types and of the normal liver parenchyma would be different. We aimed to differentiate the HC types with *SI*, and acceptibility of elastography with interobserver performance. There is no published article about USG elastography in HC, thus our article, being the first, is an important one. The goal of this study was to present the *SI* of HC in radiological databases and to support future studies.

Material and Methods

Institutional review board approval and written informed consents were obtained for this study. There was no conflict of interest in the presented study. This study was conducted between November 2013 and March 2014.

A total of 33 patients with HC were included. The inclusion criteria were: clinical diagnosis of HC and any type of HC. The exclusion criteria were: a simple cyst or non-diagnosed HC of type I and any other liver disease affecting the normal parenchyma.

The USG measurements and USG elastography were carried out by two radiologists (MD and MG, O1 and O2 respectively), with over 8 years of experience in abdominal USG. The radiologists did not see the openion of one another. Each radiologist used ROIs of two sizes (4 mm and 8 mm in diameter). Toshiba Aplio XG (SSA 790A, Toshiba Medical Systems, Nasushiobara, Japan) USG device equipped with a 5–17-MHz convex transducer was used.

Tissue strains of the HC and normal liver parenchyma were calculated quantitatively using the Elasto-Q programme (Pegasus Imaging) of Aplio XG. Elastography was performed after a routine abdominal USG evaluation. Elastography was started by selecting the 'Elast' mode using the 'Elast' button on the device. Compression and decompression with a USG probe was started after activating the elast mode. It was important that the compression in elastography was not too strong and not too weak, to obtain symmetrical sinusoidal waves. Sinusoidal waves could be followed at the bottom of the screen. The compression was applied periodically, with paying attention to symmetrical sinusoidal waves. If symmetrical waves could not be obtained, the examination was repeated. In the sinusoidal wave, the compression phase was above the baseline and the decompression phase was below the baseline. The *SI* measurements were done in the decompression phase. Decompression was more reliable because it was less affected by unbalanced compression. After an ideal sinusoidal wave was obtained we froze the image. Then, an ROI was drawn. In Types I, II and III, the cyctic component was dominant, while in Types IV and V, the solid component was dominant. In Types I, II and III we paid attention to adjust the ROI to the cystic component and in Type IV and V to the solid component but that solid component usually showed a heterogeneous echo pattern. In the application of the device, a 4-mm ROI was adjusted. If the operator did not change the ROI size, the 4-mm size of ROI was used in every case. The reference ROI was adjusted to the center of the cyst and the second ROI was adjusted to the normal liver parenchyma (Figures 1, 2). The ROIs supplied the operators with the quantitative values of the *strain* with graphic and roman numericals on the right side

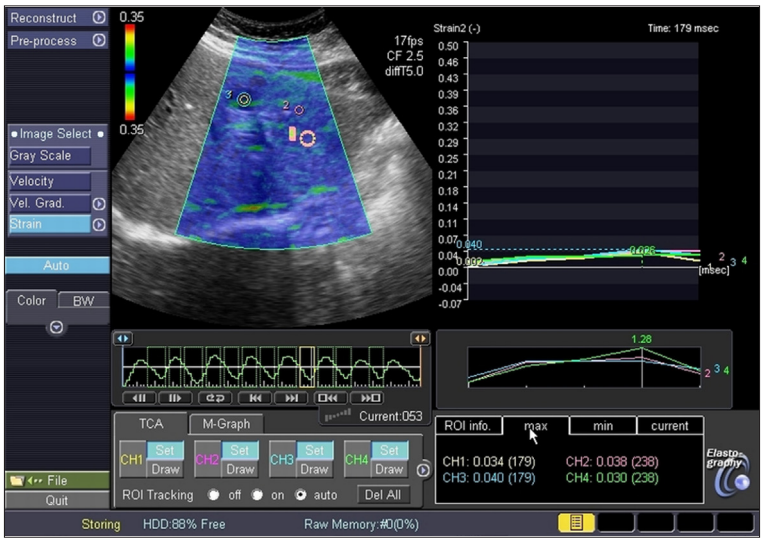

Figure 2. The image shows an ultrasound screen while the elastography programme is active. In the center of the screen, gray-scale USG image and color-coded elastography of the liver and type I Hydatic Cyst (HC) are seen. There are four different circles in the color-coded region which are the regions of interest (ROI). The smaller ones are 4 mm and the larger ones are 8 mm in diameter. The ROIs have numbers. Number 1 indicates 4 mm-ROIs in HC (reference ROI), number 2 indicates 4-mm ROIs in the normal liver parenchyma, number 3 indicates 8-mm ROIs in HC and number 4 indicates 8-mm ROIs in the normal parenchyma. Under the liver image, there is a regular sinusoidal wave. This wave shows the compression and decompression phases of the probe. The compression phase is above the baseline and the decompression phase is below the baseline. In this image the measurements are obtained in the fifth decompression phase. There are four boxes under the wave, where applications of ROI are set. On the right side of the screen, there are two graphics indicating the numerical values of the strains obtained with the ROI. Four lines belong to four ROIs. Under the graphic line there are roman numericals seen in the black box. These are numerical values of the strains. We used these numbers in the statistical analysis.

Table 1. Wilcoxon test shows the p values of the interobserver measurements and different sized ROI measurements of *Strain Index (SI)*. 'SI 1–4 mm' indicates *SI* measurement of observer 1 for 4 mm ROI. 'SI 1–8 mm' indicates *SI* measurement of observer 1 for 8 mm ROI. 'SI 2–4 mm' indicates *SI* measurement of observer 2 for 4 mm ROI. 'SI 2–8 mm' indicates *SI* measurement of observer 2 for 8 mm ROI.

b	SI 18 mm – SI 14 mm	SI 28 mm – SI 24 mm	SI 24 mm – SI 14 mm	SI 28 mm – SI 18 mm
Z	–1.456*	–2.403*	–1.459**	–.430*
P	.145	.016	.145	.667

* Based on negative ranks; ** Based on positive ranks.

of the screen. The same protocol was applied for ROI size of 8 mm. The *SI* was calculated automatically by the elastography software of the USG device using the ratio of the strain of normal parenchyma and lesion (HC in this study).

Statistical analysis

IBM SPSS version 21 was used for all the statistical analyses (IBM® SPSS® Statistics 21, © Copyright IBM Corporation 1989, 2012. US). Descriptive statistics were used for demographic data. One-Sample Kolmogorov-Smirnov test was performed to analyze the distribution of the data. The normality of the data distribution was nonparametric. Wilcoxon test was used to determine the differences in *SI*, between O1 and O2 (interobserver) and between ROI sizes of 4 mm and 8 mm. One-Way ANOVA and Post-hoc Dunnett's T3 tests were used to calculate the *SI* differences of HC types for observers and ROIs. Spearman's rho correlation coefficient was used for calculating correlations between *SI* and HC types. And we also used Wilcoxon test for each HC type for observers and ROI sizes.

Continuous variables were expressed as arithmetical mean ± standard deviation. Categorical variables were expressed as percentages (%). Level of significance was set at $p \leq 0.05$.

Results

A total of 26 out of 33 patients were female, and seven were male. The mean age was 38.85±17.62 years (range from 10 to 72 years). The distribution of the HC type was as follows: six patients with type I, II and III each, 11 with type IV, and four with type V.

There was no significiant difference in *SI* of HC (regardless of types) between O1 and O2 and between 4-mm and 8-mm ROIs ($p>0.05$) (Table 1).

We also studied the *SI* values of HC types (Table 2, Figure 3). There was no statisticially significant difference in *SI* of HC types between observers (O1–O2) and ROI sizes (4–8 mm) ($p>0.05$) (Table 3). Spearman Correlation revealed a positive sided low correlation between *SI* and HC types in different observers and ROI sizes. A higher correlation

Table 2. The *Strain Index (SI)* values of Hydatid Cyst types according to observers. 'SI 1–4 mm' indicates *SI* measurement of observer 1 for 4 mm region of interest (ROI). 'SI 1–8 mm' indicates *SI* measurement of observer 1 for 8 mm ROI. 'SI 2–4 mm' indicates *SI* measurement of observer 2 for 4 mm ROI. 'SI 2–8 mm' indicates *SI* measurement of observer 2 for 8 mm ROI.

N=33	Type I (n=6)	Type II (n=6)	Type III (n=6)	Type IV (n=11)	Type V (n=4)
SI 1–4 mm	0.91±0.39	4.81±4.13	4.41±2.70	5.59±5.38	7.27±11.85
SI 1–8 mm	2.96±2.34	13.86±17.04	5.44±3.23	4.68±3.98	3.93±2.71
SI 2–4 mm	3.01±4.29	3.07±3.10	5.40±8.40	3.17±2.41	2.30±1.69
SI 2–8 mm	9.1±12.3	3.45±3.06	29.9±37.9	4.59±3.87	6.35±7.60

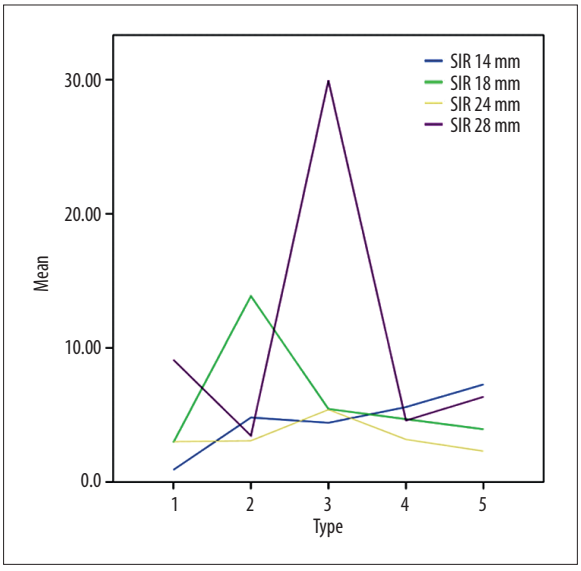

Figure 3. The graphic line of *Strain Index (SI)* based on HC types. 'X' axis indicates the HC types (Type I, II, II, IV and V) and 'Y' axis indicates the mean *SI* for both observers and two sizes of the regions of interest (ROI). Colors indicate the measurements of two observers with two different ROI sizes. The 'SI 1–4 mm (blue line)' indicates *SI* of Observer 1 for the 4-mm ROI. 'SI 1–8 mm (green line)' indicates *SI* of Observer 1 for the 8-mm ROI. 'SI 2–4 mm (yellow line)' indicates *SI* of Observer 2 for the 4-mm ROI. 'SI 2–8 mm (purple line)' indicates *SI* of Observer 2 for the 8-mm ROI.

coefficient was in 4-mm ROIs (Correlation Coefficient was 0.267 and 0.104 for observer 1 and 2, respectively) (Table 4). Almost neither of the *SI* values of each type showed any significance between observers and ROI sizes (Table 5).

Discussion

Elastography is a technique revealing relative tissue stiffness. USG elastography is a new and developing modality that is the subject of active research for clinical applications and is based on the comparison of signals acquired before and after tissue displacement. The first clinical applications were on tissues easy to displace, such as breast, thyroid, soft tissue, prostate and blood vessels. After obtaining promising results through the clinical application of USG elastography on these tissues, more recent studies focused on internal organs and liver in particular, as it was the most compelling organ, being easy to displace.

The initial USG elastography studies on the liver were based on diffuse parenchymal involvement of the liver such as fibrosis. Bota et al. published an article on Acoustic Radiation Force Impulse (ARFI) elastography in liver fibrosis. A total of 415 patients were evaluated in that study and a strong correlation was found with fibrosis and ARFI measurements ($r=0.722$, $p<0.0001$) [13]. In a study conducted by Koizumi et al., liver stiffness was measured with real-time tissue USG elastography in 70 patients with chronic hepatitis C. The results were compared with clinical assessments of fibrosis using histological stages as the reference standard. The study concluded that real-time tissue sonoelastography could be used to evaluate liver fibrosis in patients with chronic hepatitis C [14].

There are also many kinds of nodular lesions in the liver (hemangiomas, focal nodular hyperplasia, hepatocellular carcinoma, metastasis) and many imaging modalities (CT, magnetic resonance imaging, USG, Doppler USG, and also nowadays USG elastography) to obtain images and to make a differentiaton. These lesions show similarity in imaging procedures [15,16]. Differentiating benign and malignant liver lesions via imaging modalities is essential to avoid interventional procedures such as biopsy. There are a few studies on USG elastography in liver parenchyma and focal liver lesions in the literature [12,17,18]. Thereafter, liver USG elastography studies focused on focal liver masses. In a study published by Onur et al. [12] 82 patients with 93 different strain index values of focal lesions were studied to differentiate benign and malignant liver masses. The results of the study indicated that liver USG elastography could be helpful for differentiating benign and malignant liver masses. They also reported that there was an overlap between strain index values of benign and malignant liver masses. In the paper of Yu et al. [18] 89 patients and 105 liver masses were evaluated, and they reported that ARFI elastography might help to differentiate benign masses from metastases. The study of Park et al. bears some similarities with other studies on USG elastography. Similarly to Yu et al., Park et al. also used the ARFI technique for elastography. They also reported that ARFI elastography provides us with some extra information for the differential diagnosis of liver masses with some overlaps in ARFI values [17]. With these promising studies on focal liver masses, the present study aimed to evaluate USG elastography findings of HC, which is very common in the Caucasion region of Turkey.

The ARFI method was used in the studies of Yu et al. [17] and Park et al. [18]. There are different types of USG

Table 3. One-Way ANOVA test was performed to determine the significance of the *Strain Index (SI)* between HC types. 'SI 1–4 mm' indicates observer 1 using 4 mm ROI. 'SI 1–8 mm' indicates observer 1 using 8 mm ROI. 'SI 2–4 mm' indicates observer 2 using 4 mm ROI. 'SI 2–8 mm' indicates observer 2 using 4 mm ROI.

One-Way ANOVA						
SI 1–4 mm	Between groups	121.765	4	30.441	1.021	**.414**
	Within groups	834.941	28	29.819		
	Total	956.705	32			
SI 1–8 mm	Between groups	464.624	4	116.156	1.898	**.139**
	Within groups	1713.481	28	61.196		
	Total	2178.105	32			
SI 2–4 mm	Between groups	30.900	4	7.725	.386	**.817**
	Within groups	560.574	28	20.020		
	Total	591.474	32			
SI 2–8 mm	Between groups	3020.688	4	755.172	2.637	**.055**
	Within groups	8017.543	28	286.341		
	Total	11038.231	32			

Table 4. Spearman Correlation reveals positive sided low correlation between *Strain Index (SI)* and HC types in different observers and ROI sizes. The higher correlation coefficient was in 4 mm ROI. 'SI 1–4 mm' indicates *SI* of Observer 1 for 4 mm ROI. 'SI 1–8 mm' indicates *SI* of Observer 1 for 8 mm ROI. 'SI 2–4 mm' indicates *SI* of Observer 2 for 4 mm ROI. 'SI 2–8 mm' indicates *SI* of Observer 2 for 8 mm ROI.

			SI 1–4 mm	SI 1–8 mm	SI 2–4 mm	SI 2–8 mm
Spearman's rho	Type	Correlation coefficient	.267	.003	.104	–.003
		Sig. (2-tailed)	.132	.985	.565	.986
		N	33	33	33	33

** Correlation is significant at the 0.01 level (2-tailed).

elastography based on the working principle. These types are strain wave, ARFI, shear wave, and transient elastography, all having their advantages and disadvantages. Strain wave elastography allows for measurements in ascites, which is not possible with ARFI, transient or shear wave elastography. Strain wave elastography presents semiquantitative values and shows operator dependency while ARFI, transient and shear wave elastography present quantitative values and are not operator-dependent [7]. In our study we used strain elastography and did not find any significant difference between the observers. Thus, we may conclude that strain elastography presents objective values for cystic (Type I, II and III) and solid (Type IV and V) lesions of the liver.

The differential diagnosis of HC includes biliary cystadenoma, pyogenic liver abscess, cystic metastases, and hemorrhagic or infected cysts [19]. Perhaps the future research studies on elastography in cystic lesions will help to diagnose and differentiate these cystic lesions from each other. Type I HC has also a similar echo patern to a simple cyst [20,21]. The elastography value of the cysts is zero in shear-wave elastography [22]. Type I HC evolves into higher types due to its internal component. The internal component of type I HC and of a simple cyst is different. Perhaps USG elastography study can provide the medical databases with strain values to differentiate simple cysts and type I HCs.

We expected an increase in *SI* with HC types due to their increasing density. Type I is pure cystic and type V is pure calcific, thus there are really significant differences concerning the morphological component of the types. As concerns *SI* values we detected the highest correlation with the 4-mm ROI size, and observer 1 using 4-mm ROI graphic line gave us what we expected. There was an increasing line based on the types, which was noticed for observer 1 using the 4-mm ROI (Figure 3). We assumed that no significant *SI* values among HC types resulted from some limitations, such as: not enough density differences among HC types, heterogeneous internal component of HC types (except for type I and V) and limitations of USG elastography in cystic lesions.

Type I and type V have a homogenous internal component. Type I is pure cystic and type V pure calcific, but the rest of the types have a heterogeneous internal component. Thus, the location in which the ROI is adjusted affects the measurement. Type 4 is very heterogenous so it is extremely important to adjust the ROI where you want to measure it. Adjusting the ROI to either the cystic or the

Table 5. Wilcoxon test result of each type. 'SI 1–4 mm' indicates *Strain Index (SI)* of Observer 1 for 4 mm region of interet (ROI). 'SIR 1–8 mm' indicates *SI* of Observer 1 for 8 mm ROI. 'SI 2–4 mm' indicates *SI* of Observer 2 for 4 mm ROI. 'SI 2–8 mm' indicates *SI* of Observer 2 for 8 mm ROI.

	SI 18 mm – SI 14 mm	SI 28 mm – SI 24 mm	SI 24 mm – SI 14 mm	SI 28 mm – SI 18 mm
Type I				
Z	–1.992*	–1.153*	–2.023*	–.734*
Asymp. Sig. (2-tailed)	**.046**	.249	**.043**	.463
Type II				
Z	–.734*	–.524*	–.524**	–1.363**
Asymp. Sig. (2-tailed)	.463	.600	.600	.173
Type III				
Z	–.524*	–2.201*	–.943**	–1.572*
Asymp. Sig. (2-tailed)	.600	**.028**	.345	.116
Type IV				
Z	–.178*	–.578*	–1.778**	–.459**
Asymp. Sig. (2-tailed)	.859	.563	.075	.646
Type V				
Z	.000#	–.365*	–.365**	–.365*
Asymp. Sig. (2-tailed)	1.000	.715	.715	.715

* Based on negative ranks; ** Based on positive ranks; # The sum of negative ranks equals the sum of positive ranks.

solid component will change the result. In the light of this knowledge, 'the heterogeneity and the ROI location' is one of the reasons of decreasing *SI* values from type III to type IV. We always try to adjust the ROI to the solid component but sometimes it is not possible to avoid the cystic component, especially with 8-mm ROIs. Thus, the reliability of the measurements with 8-mm ROIs is lower than with the standard-applied 4-mm ROIs. The limitation of USG elastography in cystic lesions follows from serial compression intensity; the higher the intensity, the higher the tension of the internal fluid, characterizing the lesion as solid [23]. With more patients with homogenous HC type and with a higher number of patients, the *SI* values can become statistically significant, even with a substantial overlap. Despite the substantial overlap of *SI* values we still believe that liver USG elastography together with other imaging modalities can be helpful in detecting HC types, which is very important for HC treatment options. Most of the lines, except for '*SI* observer 1 using the 4-mm ROI' did not show us what we expected. But there was no singificant difference between the observers and ROI sizes.

Conclusions

In this study we used strain elastography and obtained reliable results especially for 4-mm ROIs. Not only ARFI but also strain elastography should be used in liver lesions.

HCs of type I and simple cysts have similar sonographic appearence. They should be differentiated from each other because the treatment and the follow-up is definitely different. Perhaps elastography will reveal the SI values of these cysts and the operator will be able to differentiate these lesions using elastography.

The correlation between the *SI* and types is reliable in standard-applied 4-mm ROIs. There was no statistically significant difference between the observers in *SI* values. Thus, the elastography tecnhnique is objective for HC but not appropriate to differentiate the types.

Conflict of interest

All the authors declare that there is no conflict of interest or funding support.

References:

1. Gharbi HA, Hassine W, Brauner MW, Dupuch K: Ultrasound examination of the hydatic liver. Radiology, 1981; 139: 459–63
2. Garra BS: Elastography: Current status, future prospects, and making it work for you. Ultrasound Q, 2011; 27: 177–86
3. Ophir J, Cespedes I, Ponnekanti H et al: Elastography: A quantitative method for imaging the elasticity of biological tissues. Ultrason Imaging 1991; 13: 111–34
4. Orman G, Ozben S, Huseyinoglu N et al:Ultrasound elastographic evaluation in the diagnosis of carpal tunnel syndrome: Initial findings. Ultrasound Med Biol, 2013; 39: 1184–89

5. Das D, Gupta M, Kaur H, Kalucha A: Elastography: The next step. J Oral Sci, 2011; 53: 137–41
6. Wells PN, Liang HD: Medical ultrasound: Imaging of soft tissue strain and elasticity. J R Soc Interface, 2011; 8: 1521–49
7. Onur MR, Göya C: Ultrasound elastography: Abdominal applications. Türkiye Klinikleri J Radiol-Special Topics, 2013; 6: 59–69
8. Menzilcioglu MS, Duymus M, Gungor G et al: The value of real-time ultrasound elastography in chronic autoimmune thyroiditis. Br J Radiol, 2014; 87: 20140604
9. Menzilcioglu MS, Duymus M, Citil S et al: Strain wave elastography for evaluation of renal parenchyma in chronic kidney disease. Br J Radiol, 2015; 88: 20140714
10. Dyvorne HA, Jajamovich GH, Besa C et al: Simultaneous measurement of hepatic and splenic stiffness using MR elastography: Preliminary experience. Abdom Imaging, 2015; 40: 803–9
11. Huang Z, Zheng J, Zeng J et al: Normal liver stiffness in healthy adults assessed by real-time shear wave elastography and factors that influence this method Ultrasound Med Biol, 2014; 40: 2549–55
12. Onur MR, Poyraz AK, Ucak EE et al: Semiquantitative strain elastography of liver masses. J Ultrasound Med, 2012; 31: 1061–67
13. Bota S, Sporea I, Sirli R et al: Factors that influence the correlation of acoustic radiation force impulse (ARFI), elastography with liver fibrosis. Med Ultrason, 2011; 13: 135–40
14. Koizumi Y, Hirooka M, Kisaka Y et al: Liver fibrosis in patients with chronic hepatitis C: noninvasive diagnosis by means of real-time tissue elastography – establishment of the method for measurement. Radiology, 2011; 258: 610–17
15. Brancatelli G, Baron RL, Peterson MS, Marsh W: Helical CT screening for hepatocellular carcinoma in patients with cirrhosis: frequency and causes of false-positive interpretation. Am J Roentgenol, 2003; 180: 1007–14
16. Oliver JH III, Baron RL: Helical biphasic contrast-enhanced CT of the liver: Technique, indications, interpretation, and pitfalls. Radiology, 1996; 201: 1–14
17. Park H, Park JY, Kim do Y et al: Characterization of focal liver masses using acoustic radiation force impulse elastography. World J Gastroenterol, 2013; 19: 219–26
18. Yu H, Wilson SR: Differentiation of benign from malignant liver masses with Acoustic Radiation Force Impulse technique. Ultrasound Q, 2011; 27: 217–23
19. Mortele KJ, Ros PR: Cystic focal liver lesions in the adult: differential CT and MR imaging features. Radiographics, 2001; 21: 895–910
20. Caremani M, Lapini L, Caremani D, Occhini U: Sonographic diagnosis of hydatidosis: The sign of the cyst wall. Eur J Ultrasound, 2003; 16: 217–23
21. Oruc E, Yildirim N, Topal NB et al: The role of diffusion-weighted MRI in the classification of liver hydatid cysts and differentiation of simple cysts and abscesses from hydatid cysts. Diagn Interv Radiol, 2010; 16: 279–87
22. Athanasiou A, Tardivon A, Tanter M et al: Breast lesions: Quantitative elastography with supersonic shear imaging – preliminary results. Radiology, 2010; 256: 297–303
23. Fleury EdFC, Rinaldi JF, Piato S et al: Apresentação das lesões mamárias císticas à ultra-sonografia utilizando a elastografia. Radiologia Brasileira, 2008; 41: 167–72 [in Portuguese]